Numerical study of polarisation-selective side-illuminated pin photodetectors grown on InP substrate for hybridisation on silicon platform

V. Magnin, J. Harari and D. Decoster

Abstract: A monolithic polarisation-selective side-illuminated pin photodetector is described using the coupling properties of symmetric and asymmetric slab optical waveguides. First, a basic structure is proposed, analysed and optimised by modal analysis, leading to a computed polarisation ratio of 15.7 dB. Then the symmetric waveguide is replaced by a multimode diluted waveguide optimised by a genetic algorithm coupled to a beam propagation method. This significantly improves the performance of the device and particularly the computed polarisation ratio, which reaches 21 dB. This InP-based photodetector is suitable for hybridisation on a silicon platform and is compatible with 10 Gbit/s operation.

1 Introduction

Optical communication systems generally require optical polarisation-insensitive photodetectors. Nevertheless, high speed optical systems have begun to utilise optical polarisation, either to double bandwidth by polarisation multiplexing [1, 2], or to optimally recover the signal, as in polarisation-mode dispersion mitigation techniques [3] and in coherent receivers [4]. Such systems could take advantage of the monolithic integration of polarisation filtering and photodetection functions. Some solutions have already been proposed, such as compressive strained multiquantum wells to absorb selectively TE-polarised light [5] or gold deposition to phase mismatch TM polarisation [6]. Knowing that asymmetric waveguiding structures can present a resonant behaviour depending on optical polarisation [7], we present a study of the coupling properties of symmetric and asymmetric optical waveguides and how they could be used to obtain high polarisation selectivity. A basic structure using two guiding layers is first studied. Then it is shown that a multimode diluted waveguide [8, 9] could improve the performances of that kind of device. The resulting component is suitable for hybridisation on a silicon platform [8].

2 Basic structure

The basic structure is shown in Fig. 1. Before considering the whole structure, we focus on some properties of isolated slab optical waveguides. The cut-off thicknesses of their TE guided modes are given by [10]:

$$t_m = \frac{\lambda\left(m\pi + \arctan\left(\left(n_2^2 - n_0^2\right)^{\frac{1}{2}}\left(n_1^2 - n_2^2\right)^{-\frac{1}{2}}\right)\right)}{2\pi\sqrt{\left(n_1^2 - n_2^2\right)}} \quad (1)$$

where λ is the wavelength, n_0 is the superstrate index, n_1 is the optical index of the guiding layer, n_2 is the substrate index and m can take the integer values $0, 1, 2, 3 \ldots$. Using the following data: at $\lambda = 1.55\,\mu m$, $n_2 = 3.1647$ for the InP substrate [11], $n_1 = 3.3284$ for a guiding layer made of GaInAsP lattice matched to InP with $\lambda_g = 1.18\,\mu m$ (denoted by $Q_{1.18}$ in this paper) [12], $n_0 = n_2$ for a symmetric waveguide and $n_0 = 1$ for an asymmetric one, cut-off thicknesses computed with (1) are given in Table 1. While symmetric waveguides always guide at least one mode whatever their thickness, asymmetric waveguides do not guide any mode below the cut-off thickness of the zero-order mode. Moreover, TM cut-off thicknesses being greater than TE cut-off thicknesses, as will be shown later, the asymmetric waveguides will guide TE but not TM modes if their thickness is between the two cut-offs.

This property could be used to design a TE selective photodiode, but optical injection in an asymmetric waveguide would not be optimum. A TM selective photodiode is not possible because TE cut-off thicknesses are lower than TM. Let us now consider as a whole the input guide of the structure presented in Fig. 1. This guide, of length L_g, combines a symmetric waveguide, of thickness s, to obtain good coupling with a lensed optical fibre and an asymmetric waveguide, of thickness a, to guide light near the absorbing layer. They are separated by a distance d. That input guide was studied using one-dimensional modal analysis software. Figure 2 shows the evolution of TE0 and TE1 modes for $d = 3\,\mu m$, $s = 0.15\,\mu m$ and different values of a. Up to $a = 0.31\,\mu m$ the structure has only a TE0 mode, centred on the symmetric guide. This mode is wide because the guide is thin. Around $a = 0.32\,\mu m$, the TE1 mode appears, mainly centred on the asymmetric waveguide. Its cut-off thickness is slightly greater than the value indicated in Table 1 because here the waveguide is not isolated. As a increases, the two modes more and more overlap both guides. For $a = 0.389\,\mu m$, they have two peaks centred on both waveguides and their squared modules overlap each other

IEE Proceedings online no. 20040389

doi: 10.1049/ip-opt:20040389

Paper first received 26th March and in revised form 29th October 2003

The authors are with Institut d'Electronique de Microélectronique et de Nanotechnologie (IEMN), UMR CNRS 8520-DHS-USTL, BP 69, avenue Poincaré, 59652 Villeneuve d'Ascq Cedex, France

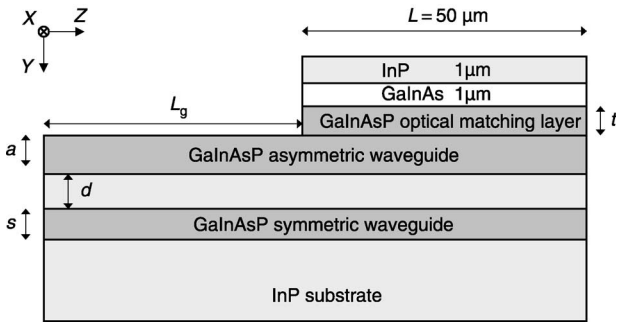

Fig. 1 *Basic structure of polarisation-selective photodiode combining input waveguide and evanescently absorbing superstructure*

Table 1: Cut-off thicknesses of TE modes at λ = 1.55 µm in symmetric and asymmetric isolated slab optical waveguides made of $Q_{1.18}$ and InP materials, computed with formula (1)

m	Symmetric t_m, µm	Asymmetric t_m, µm
0	0.000	0.297
1	0.752	1.048
2	1.503	1.800
3	2.255	2.552
4	3.007	3.304
5	3.759	4.055
6	4.510	4.807

almost exactly. Eventually, as *a* increases the TE0 mode, once centred on the symmetric guide, is now centred on the asymmetric one and *vice versa* for the TE1 mode. For TM modes, the behaviour is very similar but with *a* shifted toward greater values because the TM1 mode appears at around $a = 0.39\,\mu m$. The same kind of description could be made when higher order modes appear, by replacing TE0 and TE1 modes by the two higher order modes, the lower order modes staying mainly confined to the asymmetric waveguide. In this study we focus on the two first modes, knowing that it could be easily extended to higher modes.

Good coupling between the two waveguides occurs when beating of the two modes is optimum. The key parameter is therefore the overlap integral between modes 0 and 1 defined by:

$$I = \frac{\int E_0 \cdot E_1^*}{\sqrt{\int |E_0|^2}\sqrt{\int |E_1|^2}} \qquad (2)$$

where E_0 and E_1 are respectively the electric fields of modes 0 and 1.

Figure 3 shows the overlap integral of modes 0 and 1 against *a* for different distances *d*. The TE and TM peaks are respectively centred on $a = 0.389\,\mu m$ and $a = 0.458\,\mu m$. The gap between these two peaks is about the same as the gap between the cut-off thicknesses of TE1 and TM1 modes

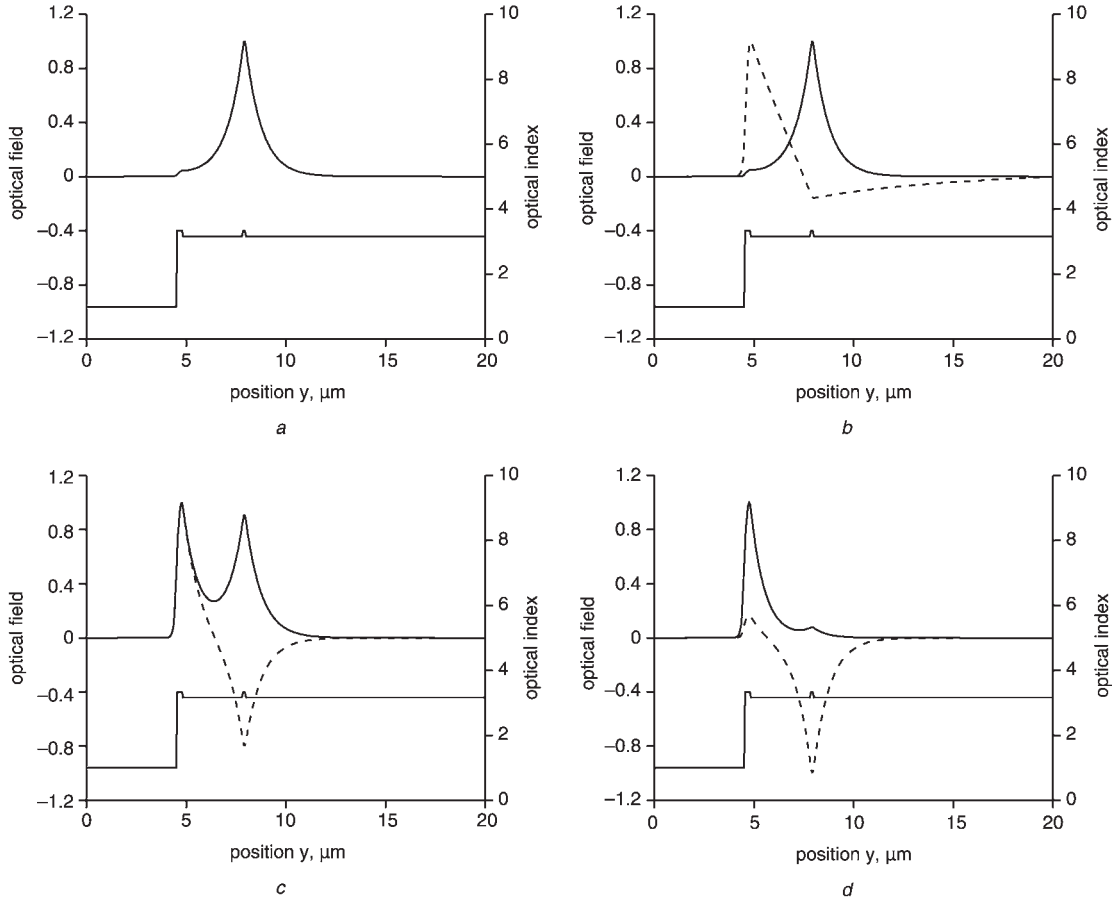

Fig. 2 *TE0 (solid line) and TE1 (dashed line) modes for $d = 3\,\mu m$, $s = 0.15\,\mu m$ and different thicknesses a of the asymmetric guide*

The optical index profile is shown as a thin solid line
a $a = 0.31\,\mu m$
b $a = 0.32\,\mu m$
c $a = 0.389\,\mu m$
d $a = 0.41\,\mu m$

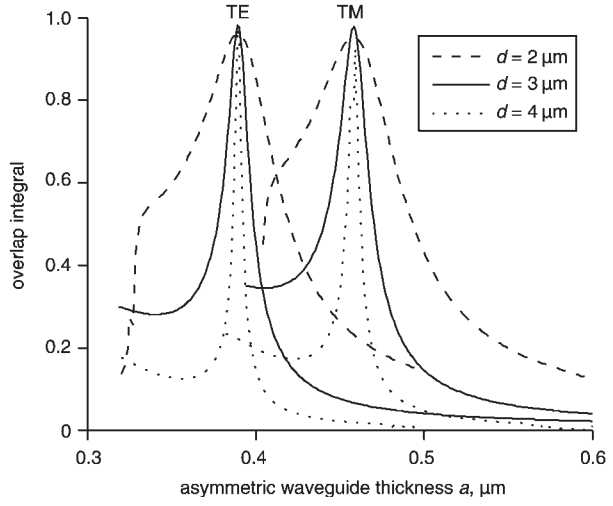

Fig. 3 *Overlap integral of modes 0 and 1 against asymmetric waveguide thickness for different distances d and s = 0.15 μm*

The left end of each curve corresponds to the cut-off thickness of mode 1

(0.32 μm and 0.39 μm). The distance d has a strong influence on the shapes of the curves. The greater the distance, the weaker the interaction between the waveguides and the narrower the peaks. The TM/TE ratios of the overlap integrals at the TM peak are 6 dB for $d = 2$ μm, 11.7 dB for $d = 3$ μm and 17 dB for $d = 4$ μm. The TE/TM ratio at the TE peak is 6.4 dB for $d = 4$ μm. For $d = 3$ μm the TM mode is just appearing and for $d = 2$ μm it does not exist. Greater d values give a greater polarisation ratio but as d increases, the difference Δn_{eff} of the effective index of 0 and 1 order modes decreases and therefore the coupling length increases rapidly as

$$L_c = \frac{\lambda}{2\Delta n_{eff}} \tag{3}$$

where λ is the wavelength. For $d = 2$ μm the resulting TE coupling length is $L_c = 150$ μm, for $d = 3$ μm $L_c = 539$ μm, and for $d = 4$ μm $L_c = 1830$ μm.

Using these results, one can design a polarisation-selective photodiode by adding an evanescent absorbing superstructure on top of the previously studied waveguide (Fig. 1). This superstructure includes a GaInAsP optical matching layer of thickness t, a 1 μm thick GaInAs absorbing layer and a 1 μm thick InP layer. Its length L is fixed at 50 μm to be compatible with 10 Gbit/s operation. A two-dimensional finite differences beam propagation method (2D-FD-BPM) with paraxial approximation was used to simulate optical beam propagation in the device [9]. The incident optical beam is assumed to be from a lensed fibre whose field diameter at 1/e is 5.8 μm at $\lambda = 1.55$ μm. The photodiode is assumed to be sufficiently wide to contain the whole propagating optical beam. This beam is initially centred on the symmetric waveguide. Figure 4 shows the simulated propagation of light in TM and TE modes with parameters $d = 3$ μm, $s = 0.15$ μm and $a = 0.389$ μm. It is clearly seen that in the TE mode (Fig. 4*a*) light is coupled from the symmetric waveguide to the asymmetric one and is absorbed by the photodiode. In the TM mode (Fig. 4*b*), no coupling occurs. Light is guided by the symmetric waveguide and propagates far below the absorbing layer. A small part of the incoming beam is diffracted directly toward the asymmetric waveguide. This explains the interference pattern standing between the two guides. In Figs. 4*c* and 4*d*, the multimode behaviour of the absorbing waveguide formed by the superstructure is

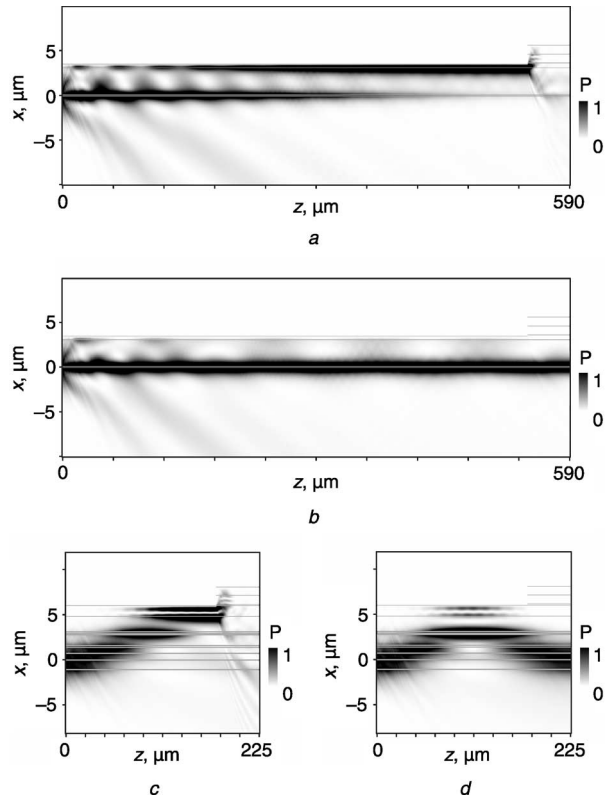

Fig. 4 *TE and TM propagation in the basic selective photodiode modelled by 2D-FD-BPM*

The vertical axis is dilated. TM and TE propagation in the multimode diluted waveguide photodiode are shown at the same scale for comparison $d = 3$ μm, $s = 0.15$ μm, $a = 0.389$ μm

a TE propagation in basic selective photodiode
b TM propagation in basic selective photodiode
c TM propagation in multimode diluted waveguide photodiode
d TE propagation in multimode diluted waveguide photodiode

obvious. The computed quantum efficiencies are 63.1% in the TE mode and 1.7% in the TM mode. These values take into account the matching losses at the input of the guide and at the beginning of the superstructure. The deduced TE/TM ratio is 15.7 dB.

3 Multimode diluted waveguide based structure

The previously studied device would be far more interesting if we could, for the same fibre, increase the polarisation ratio and the quantum efficiency while shortening the input guide. Concerning the last two points, we have recently numerically and experimentally demonstrated that a high quantum efficiency side-illuminated evanescent photodiode with a 50 μm long input guide can be obtained by including a carefully optimised multimode diluted waveguide (MDW) made of alternate InP layers and thin GaInAsP layers [8, 9]. Owing to their thickness and multimode character, MDWs exhibit complex behaviour. They can, for example, collect the optical beam from an optical fibre, bend it and focus it towards another guide. They seem difficult to analyse in modal terms but can easily be studied by a BPM. As their design involves numerous parameters and several objectives, an optimisation algorithm such as a genetic algorithm (GA) is necessary. More details on this Darwinian algorithm can be found in [9]. Having been used in [9] to obtain photodiodes with no polarisation dependence, MDW and GA will here be used to optimise a polarisation-selective photodiode.

In the present optimisation, the photodiode superstructure length L is fixed again to 50 μm and the thickness of the

GaInAs absorbing layer to 1 μm (Fig. 5). The optical beam is initially centred 5 μm below the bottom of the asymmetric waveguide. The search space is presented in Table 2. The length L_g of the input guide can range from 10 to 200 μm. All GaInAsP layers are $Q_{1.18}$ in order to make the epitaxy growth easier. The eight thin $Q_{1.18}$ layers have the same thickness but the eight corresponding InP layers have different thicknesses. The resulting number of parameters is twelve, a number easily manageable by a GA.

Having already presented a TE selective photodiode in Section 2, we now optimise a TM selective device. The two objectives of this optimisation are therefore to obtain a high quantum efficiency at 1.55-μm wavelength in the TM mode (denoted $\eta_{1.55TM}$) and a quantum efficiency in TE mode (denoted $\eta_{1.55TE}$) as low as possible, both computed by a 2D-FD-BPM coupled to the GA. First, we tested several fitness functions combining these two objectives and observed the behaviour of the algorithm and the resulting optimised devices. Eventually the following fitness function proved to be suitable:

$$f = Log\left(\frac{\sqrt{\eta_{1.55TM}}}{\eta_{1.55TE} + 0.01}\right) \quad (4)$$

Such a fitness function is quite unconventional for a GA because its values can range from minus infinity to plus infinity, but the algorithm deals easily with it because fitness values are only used to sort the population of devices from best to worst. The upper square root is giving more weight to $\eta_{1.55TM}$. The addtion of 0.01 to $\eta_{1.55TE}$ limits the weight of the TE minimisation objective. It avoids obtaining an uninteresting final device with, for example, $\eta_{1.55TE} = 0.00001\%$ and $\eta_{1.55TM} = 20\%$. The logarithm aims just to restrain the range of possible values. The GA was launched several times because stochastic characteristics of such an algorithm can lead to slightly different results at each launch. The epitaxy of the best device is shown Table 3. The length of the input guide is $L_g = 175\,\mu m$.

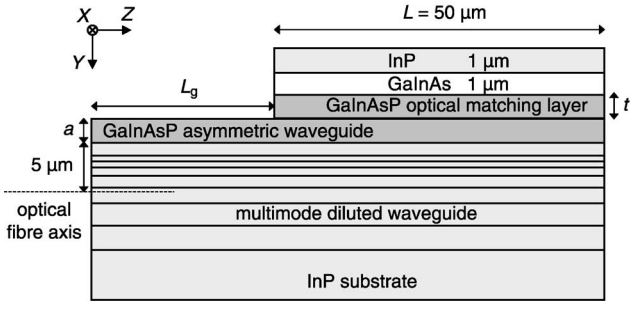

Fig. 5 *Structure of photodiode with multimode diluted waveguide*

Its quantum efficiencies are $\eta_{1.55TM} = 77.7\%$ and $\eta_{1.55TE} = 0.6\%$. These values include coupling losses. The TM/TE ratio is 21 dB. Figure 4*c* and 4*d* show the simulated propagation of light in the device, respectively, in TM and TE modes. In both cases the effect of the MDW is to bend the optical beam towards the asymmetric waveguide. We have already shown in [9] that in an infinitely long MDW guide, without absorbing superstructure, light exhibits a snake-like behaviour, moving vertically up and down with a certain spatial period due to beating of the modes. In the present device, the half-period determined by 2D-FD-BPM is approximately 175 μm in the TM mode and 110 μm in the TE mode. The input guide being 175 μm long, TM light can be easily evanescently absorbed by the photodiode superstructure, whereas TE light returns in the diluted waveguide before the beginning of the superstructure, thus passing far below the absorbing layer. Moreover the coupling between the diluted waveguide and the asymmetric one is weaker in the TE mode.

Let us compare the MDW and basic structures. The only drawback of MDW is the thickness of the epitaxial layer, here 7.16 μm without the superstructure. But the quantum efficiency in the selected polarisation is 77.7% instead of 63%, the polarisation ratio is 21 dB instead of 15.7 dB and the input guide is 175 μm long instead of 540 μm. These large improvements clearly demonstrate the interest of the MDW approach. The higher quantum efficiency is partly due to the better coupling with the optical fibre allowed by the thickness of the MDW. A modal analysis shows that there are four modes in the input waveguide and two of these modes are more than 7 μm wide. Figure 4 shows that insertion losses at the input of the superstructure are similar in both structures but that insertion losses at the input of the waveguide are far lower in the MDW structure. Concerning the unselected polarisation (here TE), the functioning of the MDW structure is quite different from that of the basic one. Light is now propagating several micrometres further from the absorbing layer. Moreover, light being injected deeper and the coupling between MDW and optical fibre being better, there is no direct injection in the asymmetric waveguide. These two points lead to far lower absorption of the unselected polarisation (0.6% instead of 1.7%).

Figure 6 shows the effect of vertical misalignment of the optical fibre on TE and TM quantum efficiencies and on the TM/TE ratio of the MDW structure. The total TM misalignment tolerance at 1/e is 2.6 μm. If the fibre is aligned too high (negative values on Fig. 6) towards the surface, TE quantum efficiency increases because light is injected directly in the asymmetric waveguide. This is the

Table 2: Twelve-dimensional search space of the genetic algorithm

Parameter	L_g (μm)	Waveguide InP thicknesses (μm)	Diluted Q1.18 thickness (μm)	Asymmetric waveguide thickness *a* (μm)	Optical matching layer thickness *t* (μm)
Min.	10	0	0.02	0	0
Max.	200	2	0.20	2	1

Table 3: Epitaxial structure of the TM photodiode

InP	GaInAs	$Q_{1.18}$	InP	$Q_{1.18}$	InP	$Q_{1.18}$	InP	$Q_{1.18}$	InP	$Q_{1.18}$	InP	$Q_{1.18}$	InP	$Q_{1.18}$	InP	$Q_{1.18}$	InP	$Q_{1.18}$	InP	$Q_{1.18}$
1	1	0.1	0.02	1.2	1.68	0.05	0.13	0.05	0.13	0.05	1.13	0.05	0.17	0.05	0.62	0.05	0.69	0.05	0.99	0.05

Thicknesses in μm; upper layers are on the left

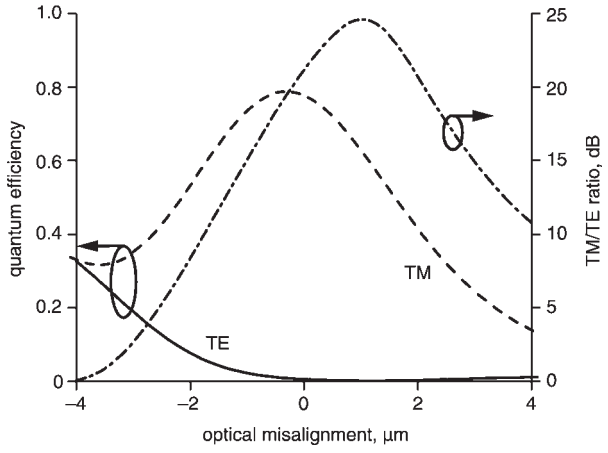

Fig. 6 *Quantum efficiencies and TM/TE ratio against vertical optical misalignment of optical fibre (2D-FD-BPM results)*
The substrate is on the right

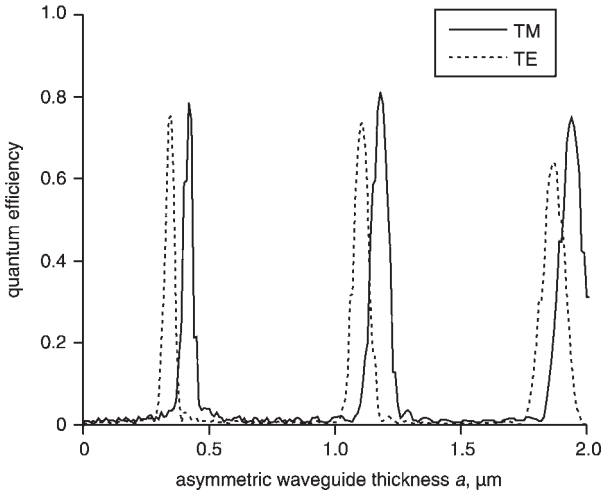

Fig. 8 *TM and TE quantum efficiencies against asymmetric waveguide thickness (3D-FD-BPM results)*

reason why the polarisation ratio falls more rapidly towards the surface than towards the substrate. So its maximum is slightly shifted towards the substrate and has a value of 24.6 dB but with only 63% TM quantum efficiency. Figure 7 shows that the misalignment tolerance of the MDW structure is slightly greater than that of the basic structure (2.6 μm instead of 2.3 μm) because its quantum efficiency is always higher.

We studied, using 3D-FD-BPM, the dependence of quantum efficiency on asymmetric waveguide thickness (cf. Fig. 8). In TM mode, the photodiode has high quantum efficiency only for certain discrete values: 0.42 μm, 1.18 μm, 1.94 μm etc. In TE mode, the peaks are shifted towards lower values: 0.35 μm, 1.11 μm, 1.87 μm etc. These values are linked to the cut-off thicknesses of the modes of the input waveguide. A first consequence of these results is that a TE selective photodiode could be obtained by changing only the thickness of the asymmetric waveguide layer. A second consequence is that the thickness and composition of this epitaxial layer must be very accurately controlled, ideally with 0.01 μm accuracy. Since it is difficult to control with such precision the growth of GaInAsP thicknesses greater than one micrometre, a solution is to replace this $Q_{1.18}$ layer by a superlattice composed from alternate InP layers and layers of higher λ_g quaternary material. Its value and the thicknesses of InP and quaternary materials can be chosen properly to obtain a mean optical index identical to the index of $Q_{1.18}$. In that way, the optical behaviour would be the same and control of the epitaxial growth would be far easier. Another practical issue could be scattering losses, a phenomenon occurring when a part of the light beam propagates near the semiconductor/air interface. This problem has not been encountered in other similar fabricated devices [8, 9].

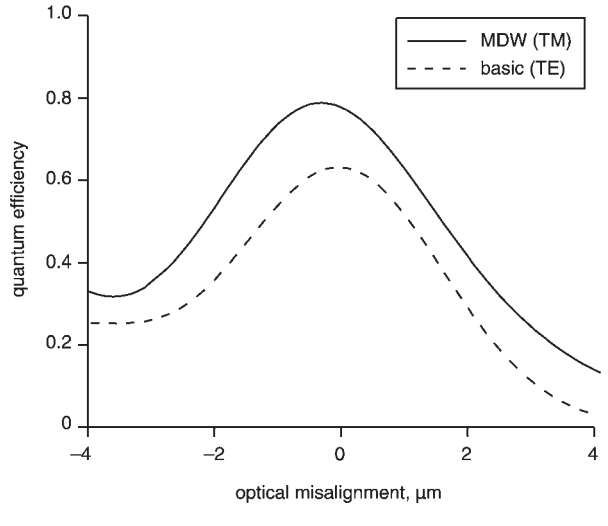

Fig. 7 *Quantum efficiencies of basic and MDW structures against vertical optical misalignment of optical fibre (2D-FD-BPM results)*
The substrate is on the right

4 Conclusions

The aim of this paper was to design a monolithic polarisation-selective side-illuminated pin photodetector compatible with 10 Gbit/s operation and hybridisation on a silicon platform. Knowing that the cut-off thicknesses of modes in a slab waveguide are different in TE and TM modes, the coupling properties of a symmetric and an asymmetric slab waveguide were studied by modal analysis. By computing the overlap integral between the two higher order modes of the proposed structure, we designed a first evanescent photodiode with a 540 μm long input guide. In TE mode light is coupled from the symmetric waveguide to the asymmetric one and the computed quantum efficiency at 1.55 μm is 63%. In TM mode no coupling occurs and the quantum efficiency is only 1.7%, resulting in a 15.7 dB polarisation ratio.

The second part of this work is based on the concept of a multimode diluted waveguide (MDW), which had already been successfully used to fabricate high efficiency evanescent photodiodes insensitive to optical polarisation. The symmetric waveguide of the first structure has been replaced by a MDW carefully optimised by a genetic algorithm coupled to a beam propagation method. The performance was thus greatly enhanced: whereas the input guide is three times shorter, the computed TM quantum efficiency is 78%, the polarisation ratio is 21 dB and the total vertical misalignment tolerance is 2.6 μm instead of 2.3 μm. A TE selective photodiode can be obtained by changing only the thickness of the asymmetric waveguide layer. Concerning the fabrication of such a device, the main difficulty will be to grow thick epitaxial layers with precise thicknesses.

Further work is in progress to determine if the same principle and method could be used to design a polarisation

diversity photodetector combining monolithically, without expitaxial regrowth, a first photodiode to detect TM modes and a second one to detect TE modes.

5 Acknowledgments

We would like to thank Louis Giraudet from ALCATEL-OPTO+ for our fruitful collaboration on multimode diluted waveguides.

6 References

1 Hinz, S., Sandel, D., Wüst, F., and Noé, R.: 'Polarization multiplexed 2 × 20 Gbit/s RZ transmission using interference detection'. Proc. Optical Fiber Communication Conf., Anaheim, CA, USA, March 2001, paper WM4

2 Kahn, J.M., and Ho, K.-P.: 'Ultimate spectral efficiency limits in DWDM systems'. Proc. Optoelectronics and Communications Conf., Yokohama, Japan, July 2002

3 Lima, A.O.: 'Polarization effects in optical communication systems, ENEE635/785B: enabling WDM technologies'. Final Report, 2001, Department of Computer Sciences and Electrical Engineering, University of Maryland Baltimore County. http://research.umbc.edu/~ychen/ee635/ENEE785BFall01Report_Lima.pdf

4 Hilbk, U., Hermes, T., Meissner, P., Westphal, F.J., Jacumeit, G., Stenzel, R., and Unterbörsch, G.: 'First system experiments with a monolithically integrated tunable polarization diversity heterodyne receiver OEIC on InP', *IEEE Photonics Technol. Lett.*, 1995, **7**, (1), pp. 129–131

5 Ferreras, A., Anton, O., Rodriguez, F., Gomez-Salas, E., de Miguel, J.L., and Hernandez-Gil, F.: 'Compressive strained multiquantum-well waveguide photodetectors for coherent receivers', *IEEE Photonics Technol. Lett.*, 1995, **7**, (5), pp. 546–548

6 Deri, R.J., Pennings, E.C.M., Scherer, A., Gozdz, A.S., Caneau, C., Andreadakis, N.C., Shah, V., Curtis, L., Hawkins, R.J., Soole, J.B.D., and Song, J.-I.: 'Ultracompact monolithic integration of balanced, polarization diversity photodetectors for coherent lightwave receivers', *IEEE Photonics Technol. Lett.*, 1992, **4**, (11), pp. 1238–1240

7 Kim, B.-G., Shakouri, A., Liu, B., and Bowers, J.E.: 'Improved extinction ratio in ultra short directional couplers using asymmetric structures', *Jpn. J. Appl. Phys. 2, Lett.*, 1998, **37**, (8A), pp. L930–L932

8 Giraudet, L., Harari, J., Magnin, V., Pagnod, P., Boucherez, E., Decobert, J., Bonnet-Gamard, J., Carpentier, D., Jany, C., Blache, F., and Decoster, D.: 'High speed evanescently coupled PIN photodiodes for hybridisation on silicon platform optimised with genetic algorithm', *Electron. Lett.*, 2001, **37**, (15), pp. 973–975

9 Magnin, V., Giraudet, L., Harari, J., Decobert, J., Pagnot, P., Boucherez, E., and Decoster, D.: 'Design, optimisation and fabrication of side-illuminated p-i-n photodetectors with high responsivity and high alignment tolerance for 1.3 μm and 1.55 μm wavelength use', *J. Lightwave Technol.*, 2002, **20**, (3), pp. 477–488

10 Hunsperger, R.G.: 'Integrated optics: theory and technology' (Springer-Verlag, New York, 1985)

11 Gini, E., and Melchior, H.: 'The refractive index of InP and its temperature dependence in the wavelength range from 1.2 μm to 1.6 μm'. Proc. 8th Int. Conf. on Indium Phosphide and Related Materials, New York, NY, USA, 1996, pp. 594–597

12 Broberg, B., and Lindgren, S.: 'Refractive index of $In_{1-x}Ga_xAs_yP_{1-y}$ layers and InP in the transparent wavelength region', *J. Appl. Phys.*, 1984, **55**, (9), pp. 3376–3381